Research Square

Preprints are preliminary reports that have not undergone peer review.
They should not be considered conclusive, used to inform clinical practice,
or referenced by the media as validated information.

Seasonality of Haemaphysalis longicornis and its implications for the transmission of severe fever with thrombocytopenia syndrome virus: a modelling study

Qu Cheng

chengqu@hust.edu.cn

Huazhong University of Science and Technology

Qi Li

Huazhong University of Science and Technology

Minghui He

Huazhong University of Science and Technology

Xiang Xu

Huazhong University of Science and Technology

Yufei Yan

Huazhong University of Science and Technology

Junhua Tian

Wuhan Center for Disease Control and Prevention

Zhihang Peng

Chinese Center For Disease Control and Prevention

Research Article

Keywords: Haemaphysalis longicornis, seasonality, severe fever with thrombocytopenia syndrome, developmental duration

Posted Date: November 24th, 2026

DOI: https://doi.org/10.21203/rs.3.rs-11002836/v1

License: This work is licensed under a Creative Commons Attribution 4.0 International License.
Read Full License

Additional Declarations: No competing interests reported.

Abstract

Background

The Asian longhorned tick, *Haemaphysalis longicornis*, is the primary vector of severe fever with thrombocytopenia syndrome (SFTS), an emerging infectious disease rapidly spreading in Asia with a case-fatality rate of up to 30%. Understanding the seasonal activity of *H. longicornis* is critical for elucidating SFTS epidemiology and improving risk prediction.

Methods

We compiled databases of life stage-specific seasonal activity data for *H. longicornis*, as well as laboratory-derived developmental durations under different temperature conditions, from the published literature. We then developed an empirical model integrating laboratory observations with field temperature data to predict interstadial and full-generation developmental durations across 20 locations with observed tick seasonality, seven SFTS transmission hotspots, and three locations without reported *H. longicornis* presence. Finally, we inferred the cohort structures underlying observed *H. longicornis* seasonal patterns by integrating observed seasonality with model-predicted developmental durations.

Results

Despite substantial variation in annual mean temperature (7.3–17.4°C), the seasonal activity of *H. longicornis* was largely synchronous across locations, with nymphs peaking in spring, adults in summer, larvae in fall, and no detectable activity during winter, potentially attributable to the substantially higher overwinter survival of nymphs than of other life stages. In contrast, human SFTS cases exhibited diverse seasonal patterns, with peaks occurring in May, July, or October depending on the location, suggesting that variation in human-tick contact patterns may play an important role in shaping the observed seasonality of human SFTS. The predicted full-generation developmental duration was 1–2 years in locations with observed *H. longicornis* seasonality or reported human SFTS cases, but < 1 year in locations without known *H. longicornis* presence under most examined scenarios. Inferred cohort structures showed that a single seasonal activity peak may comprise multiple overlapping cohorts. For example, the summer adult peak from May to August likely consists of overwintered adults for the early part, and newly matured adults that fed as nymphs in the spring for the latter part.

Conclusions

These findings highlight the need to consider human-tick contact patterns and location- and month-specific temporal scales when modelling human SFTS risk.

Background

Severe fever with thrombocytopenia syndrome (SFTS) is an emerging, potentially fatal tick-borne zoonotic disease first identified in the Dabie Mountain region of China in 2009 [1]. Since its discovery, human cases have been reported across East and Southeast Asia, including South Korea, Japan, Vietnam, Thailand, and Myanmar, with serological evidence also detected in Pakistan and Kenya [2]. SFTS poses a significant public health threat due to its high case-fatality rate ranging from 18% to 30%, the lack of effective vaccines and antiviral treatments, and its rapid geographic expansion [2, 3, 4]. China, South Korea, and Japan currently bear the highest disease burden, with all three countries reporting substantial increases in both the number of cases and the number of affected regions over the past decade. For example, China reported 71 cases across 18 counties in 2010, surging to 5,062 cases across 358 counties by 2023 [4]. South Korea reported 36 cases across 10 provinces in 2013, and 167 cases across 16 provinces in 2024 [5, 6]. Similarly, Japan reported 60 cases in 16 prefectures in 2015, rising to 191 cases across 32 prefectures by 2025 [7].

The SFTS virus (SFTSV, also known as *Bandavirus dabieense*) is transmitted to humans primarily through tick bites, though transmission can also occur through direct contact with the body fluids, particularly blood, of infected humans or animals [8]. Although a variety of tick species, including *Haemaphysalis flava*, *Rhipicephalus microplus*, and *Dermacentor sinicus*, have been found to be SFTSV-RNA positive or capable of transmitting the virus, *H. longicornis* is considered the primary vector of SFTSV, because of its dominance in SFTS-endemic regions, and higher transmission efficacy when compared to other species [3, 9, 10, 11].

Haemaphysalis longicornis inhabits a wide range of environments globally, spanning approximately 24.5–51.8 °N and 27.6–43.3 °S, where daily mean temperatures typically vary from 20 to 30°C in summer and − 20 to 12°C in winter [10]. *H. longicornis* develops through four life stages: egg, larva, nymph, and adult. Each active stage (i.e., larva, nymph, and female adult) requires a single blood meal, during which pathogens may be transmitted between hosts and ticks or between ticks. Within a year, each active stage typically exhibits one main activity peak [12, 13, 14]. Although several field surveys have documented the seasonal activity of different life stages of *H. longicornis* [12, 13, 14], these studies have largely been descriptive and geographically localized, providing limited insight into the global patterns of *H. longicornis* seasonality and the factors underlying their consistency or variation across locations. Crucially, current research fails to clarify the cohort structure underlying observed peaks, which could provide important insights into the temporal progression of SFTSV through different tick life stages. Although lipid analyses of field-collected questing ticks can provide such insights, they are often very costly [15, 16].

On the other hand, laboratory studies have established that temperature strongly affects the developmental duration of *H. longicornis* [17, 18, 19]. By integrating these laboratory-derived relationships with field temperature data using appropriate models [15, 20], interstadial (i.e., between successive life stages) and full-generation developmental durations can be predicted under natural

conditions. Understanding these durations is critical for assessing disease risk because they determine the temporal lag between environmental conditions and subsequent pathogen transmission. For example, Lyme disease is transmitted to humans primarily by nymphal *Ixodes pacificus* ticks. Since questing nymphs develop from eggs laid by adults that fed approximately three years earlier, increased host availability associated with masting events three years previously may contribute to elevated human Lyme disease risk in the current year [21]. However, no comparable understanding exists for *H. longicornis*, limiting our ability to characterize how environmental conditions in previous years may influence current SFTS risk.

In this study, we systematically compiled field survey data on stage-specific seasonal activity, together with laboratory data on the effects of temperature on the developmental durations of *H. longicornis* across different life stages. We first characterized global patterns of seasonality for each life stage of *H. longicornis*. We then used an empirical model to estimate interstadial and full-generation developmental durations across three types of locations, including those with field observations of tick seasonality, SFTSV transmission hotspots, and warm-climate areas where *H. longicornis* has not been reported. Finally, we inferred the latent cohort structure underlying the three observed seasonal activity peaks, providing a basis for determining how far back in time climatic conditions may need to be considered when assessing current human SFTS risks.

Methods

Data collection and process

Tick seasonality data under field conditions

To characterize the global seasonality of *H. longicornis* under natural conditions and infer its cohort structure, we compiled stage-specific abundance data from published field surveys. We systematically searched PubMed, Web of Science, and China National Knowledge Infrastructure (CNKI) using the keywords "*Haemaphysalis longicornis*" and ("survey" or "season"). Studies published up to September 21, 2026, were eligible for inclusion if they reported tick abundance time series covering at least one complete tick activity season at a spatial resolution equal to or finer than the first-administrative level, identified ticks to the species level, reported the abundance of questing ticks for all three active life stages, and did not involve acaricide application (Fig. S1). For each eligible study, we extracted the geographic location, survey period, and stage-specific abundance of *H. longicornis*. Data presented only in figures were extracted using WebPlotDigitizer (https://apps.automeris.io/wpd4/). Because seasonal activity was typically presented as continuous curves without showing exact sampling dates, we first interpolated the reported data to obtain daily abundance estimates for each life stage and then aggregated these estimates into monthly averages.

Laboratory data

To characterize the relationships between climatic factors and developmental durations of *H. longicornis*, we systematically searched PubMed, Web of Science, and CNKI using the keywords "*Haemaphysalis longicornis*" combined with "temperature" or "humidity" or "biological characteristics". Studies published up to September 21, 2026, that reported the duration of any developmental substage under constant temperature or humidity conditions in the laboratory were included (Fig. S1). These substages included egg incubation; larval, nymphal, and adult prefeeding and feeding; larval and nymphal premoulting; and adult preoviposition and oviposition. For each eligible study, we extracted temperature, humidity, strain type (bisexual or parthenogenetic), developmental substage, sample size, and summary statistics for developmental duration, including the mean, standard deviation, minimum, and maximum, when available. When only minimum and maximum durations were reported, we estimated the mean duration as the midpoint of the reported range. This approximation showed good agreement with reported mean durations among studies that provided both mean and range estimates (Fig. S2). Since developmental durations showed limited variation across humidity levels and data were sparse for individual strain types (Figs. S3-4), we considered only temperature, but not humidity or strain type, in subsequent analyses.

Temperature data

To estimate developmental durations under natural conditions, we obtained location-specific daily mean 2-m air temperatures from the ERA5-Land Daily Aggregated dataset via Google Earth Engine (https://earthengine.google.com/). To examine temporal changes in tick phenology in the context of global warming, we extracted temperature data for the period from 1980 to 2025.

Daylength data

Short photoperiods during fall and winter may trigger behavioral diapause of *H. longicornis*, during which ticks cease questing and feeding and remain hidden in the leaf-litter layer or topsoil [22, 23]. To explicitly account for behavioral diapause in our model, we calculated daily daylength at each study location based on latitude and day of year, following the algorithm proposed by Forsythe et al. [24].

Human SFTS cases

To examine the implications of tick seasonality and cohort structure for SFTSV transmission, we compiled the monthly proportion of reported human SFTS cases for each first-level administrative division in mainland China, South Korea, and Japan. For each administrative division, the proportion of cases in a given month was calculated as the number of cases reported in that month divided by the total number of cases reported over the entire study period. Human case data were obtained from the Chinese Center for Disease Control and Prevention for mainland China (2011–2023), the Infectious Disease Surveillance Yearbook for South Korea (2014–2022, https://dportal.kdca.go.kr/), and the Infectious Disease Information Website for Japan (2014–2022, https://id-info.jihs.go.jp/). The temporal

coverage varied across countries due to differences in data availability. We further calculated SFTS incidence rates for each first-level administrative division for each country using 2018 population data, representing the approximate midpoint of the SFTS case data, sourced from the National Bureau of Statistics (province level, https://data.stats.gov.cn/) for China, the Korean Statistical Information Service (KOSIS, prefecture level, https://kosis.kr/eng/) for South Korea, and e-Stat (prefecture level, https://www.e-stat.go.jp/en/regional-statistics/ssdsview/prefectures) for Japan.

Study locations

Our study sites primarily comprised locations with published field surveys of the seasonality of *H. longicornis*. To complement these, we included seven additional locations with high SFTS incidence rates but no field data on *H. longicornis* seasonality (i.e., Dalian, Xinyang, and Taizhou in China, Hwacheon and Jeju in South Korea, and Miyazaki and Hiroshima in Japan) and three additional warm-climate locations (i.e., Guangzhou, Nanning, and Haikou in China) where *H. longicornis* presence has not been documented [10]. These locations were included to examine whether their developmental durations differed from known *H. longicornis* habitats. Interstadial and full-generation developmental durations were predicted for all locations using local temperature and daylength data; however, underlying cohort structures were not inferred for the ten additional locations due to the absence of seasonal activity field observations.

Characterizing the relationships between temperature and developmental durations under laboratory conditions

Since the prefeeding and feeding durations across all three tick life stages showed little variation with temperatures, we treated both as constants and estimated their means and standard deviations from eligible studies. Conversely, the remaining temperature-dependent developmental substages, including incubation, premoulting, preoviposition, and oviposition, were modeled using exponential functions following previous studies as $y = ae^{bx}$ [15, 20], with temperature as the independent variable and developmental durations as the dependent variables.

Estimation of interstadial developmental durations under field conditions

We estimated the developmental durations from larva to nymph, nymph to adult, and adult to larva for each month, initiated at the midpoint of the month. Since eggs do not feed and their seasonality cannot be directly observed in the field, the egg stage was not explicitly modeled. The larva-to-nymph and nymph-to-adult transitions comprised questing, feeding, premoulting, and prefeeding, whereas the adult-to-larva transition comprised questing, feeding, preoviposition, oviposition, egg incubation, and prefeeding (Table S1). To enable standard comparisons across locations unbiased by year-to-year weather anomalies, we used the average daily mean temperatures from 2021 to 2025 to characterize

interstadial developmental durations. However, year-specific field temperatures were used when inferring underlying cohort structures.

To account for uncertainty, we estimated each interstadial developmental duration 1,000 times by summing the durations of the corresponding substages randomly sampled 1,000 times from specific distributions. For temperature-independent developmental durations (i.e., prefeeding and feeding), we sampled from truncated normal distributions using the means and standard deviations estimated from laboratory studies, with a lower bound of 1 day (Table S1). For temperature-dependent developmental durations (i.e., premoulting, preoviposition, oviposition, and incubation), directly sampling from the fitted temperature-developmental duration functions would be inappropriate, because temperatures vary daily under natural conditions, unlike the constant temperatures set in laboratory experiments. Instead, we adopted the approach of Randolph et al. [15, 20]. Specifically, for each day, we calculated the daily development proportion as the reciprocal of the developmental duration predicted at the day's temperature. We then defined the total development duration as the number of days required for the cumulative daily development proportion to first exceed 1 (Table S1). Based on the literature [15] and our compiled laboratory data for *H. longicornis*, the standard deviations of temperature-dependent developmental durations were typically 5–10% of their means. We therefore sampled these durations from truncated normal distributions with the means given by the cumulative-development approach described above, standard deviations equal to 10% of the means, and a lower bound of 1 day. Questing duration was modeled using a truncated normal distribution with a mean of 22 days, a standard deviation of 10 days, and a lower bound of 5 days, following previous studies on several *Ixodes* tick species [15, 20], because no data on questing duration of *H. longicornis* were available. We also conducted sensitivity analyses using alternative mean durations of 12, 32, or 42 days. The lower and upper bounds were informed by field observations from Xiaowutai, China, where both seasonal activity patterns and monthly observations of nymph-to-adult developmental durations (from feeding to premoulting, excluding questing duration) have been reported [12, 25]. The intervals between the peaks of nymphal and adult activity were both approximately 85 days in 2008 and 2009, with nymphal activity peaking around April 15 and adult activity around July 8. The reported nymph-to-adult developmental duration, excluding questing duration, was 69.4 days for development initiated in April, implying a questing duration of approximately 15.6 days. To establish a conservative upper bound that accommodates scenarios in which the nymph-to-adult developmental duration is relatively short, we used the reported duration of 42.5 days for development initiated in May, yielding an estimated questing duration of 42.5 days.

As a partial validation, we compared our predicted interstadial developmental durations with observations reported for Xiaowutai, China [12]. Since that study reported only monthly average temperatures, we approximated daily temperatures by assigning each monthly mean temperature to the midpoint of the corresponding month and linearly interpolating daily temperature between these midpoint values.

Estimation of full-generation developmental durations under field conditions

We estimated the duration of a complete tick generation under field conditions for nymph cohorts initiating questing on the 1st, 11th and 21st days of each month. Nymphs were chosen as the starting stage because they are typically the first active life stage observed each year (Fig. 1B). The full-generation developmental duration was calculated by sequentially summing the interstadial developmental durations from nymph to adult, then adult to larva, and larva to nymph. Importantly, the full-generation developmental duration for a cohort initiated in a given month does not equal the simple sum of the three static interstadial developmental durations starting from the same month, since in the full-generation calculation, each successive life stage progresses sequentially under dynamically changing temperatures, whereas interstadial calculations assume all three stages initiate simultaneously in the same month.

We incorporated behavioral diapause during winter, when ticks become inactive and shelter in leaf litter and topsoil to avoid harsh climatic conditions and limited host availability [22, 23]. We defined the photoperiod thresholds for diapause onset and termination based on the daylength when approximately half of the ticks were active in a previous field experimental study [22]. The resulting thresholds were 12.5 and 11.5 hours of daylength for diapause termination and onset, respectively. Across all study locations with H. *longicornis* or reported human SFTS cases, these thresholds corresponded to March 30-April 5 (mean: March 31, the 90th day of a year) and October 10–17 (mean: October 11, the 284th day of a year), respectively (Fig. S5). To assess the robustness of our results to uncertainty in these thresholds, we conducted sensitivity analyses using alternative daylength thresholds of 11.5 and 13.5 hours for diapause termination and 10.5 and 12.5 hours for diapause onset. Both the baseline and alternative thresholds were selected based on the seasonal occurrence of *H. longicornis* across locations with available field data on tick seasonality (Fig. S6).

To evaluate temporal changes in the full-generation developmental durations in the context of global warming, we calculated the average daily mean temperatures by decade from 1981 to 2025 (i.e., 1981–1990, 1991–2000, 2001–2010, 2011–2020, and 2021–2025), and estimated full-generation developmental durations separately for each period.

Inferring cohort structure from seasonal activity and developmental durations

To reconstruct the underlying cohort structure of each life stage of *H. longicornis* (e.g., to determine when ticks active in a given month would develop into the subsequent life stage), we combined monthly stage-specific tick abundance from eligible studies with predicted interstadial developmental durations starting from the midpoint of each month (i.e., the 15th day). For locations with multi-year observational data, we constructed a representative daily temperature profile by averaging temperatures for each calendar day across the surveyed years. This temperature profile was then used to estimate the

interstadial developmental duration for each cohort starting on the 15th day of each month. The predicted duration was added to the cohort's starting date to determine the corresponding end time of the current stage, which simultaneously marked the emergence date of the subsequent stage. In this way, the observed monthly abundance of each life stage could be linked to the expected timing of emergence of the subsequent life stage, allowing us to reconstruct the underlying cohort structure.

Results

Seasonality of H. longicornis

A total of 19 studies reporting stage-specific seasonal activity of *H. longicornis* were included (Fig. S1). Because one study reported data separately for two locations, a total of 20 locations were included in the subsequent analyses (Table S2, red dots in Fig. 1A), including eleven in South Korea (KR), four in the United States (US), three in China (CN), and two in Japan (JP). The latitude of these locations ranged from 31.8° to 40.9° N, but did not include several areas with high reported SFTS incidence rates (Fig. 1B). We therefore additionally selected several representative locations, such as Xinyang in the Dabie Mountain area and Taizhou on the eastern coast of China, Jeju Island in South Korea, and the Miyazaki and Hiroshima prefectures in Japan (orange dots in Fig. 1A), and incorporated these locations into the analyses of the interstadial and full-generation developmental durations.

Across the 20 study locations, *H. longicornis* was active from March to October, with a single main annual peak observed for each stage (Fig. 1B). Nymphs became active first, with peak activity generally occurring from March to June. The timing of the peak tended to occur slightly earlier at lower latitudes and later at higher latitudes. At several sites, including Bukhansan Dullegil, Shandong, Boso Peninsula, and Hefei, a smaller secondary peak was observed between September and October. Adults peaked subsequently, generally from May to August, with peak activity again tending to occur earlier at lower latitudes. Larvae showed the last major peak, occurring primarily from August to September, although smaller secondary peaks were observed between April and May at several sites, including Gyeonggi-do 1, Shandong, and Jeonbuk. The original stage-specific tick abundance time series for each location are shown in Fig. S7.

Relationships between temperature and developmental durations under constant laboratory conditions

A total of 16 eligible laboratory studies reporting the relationships between constant temperature or humidity and the developmental period of *H. longicornis* were identified (Fig. S1, Table S3). Most studies examined temperatures between 20 and 30°C, although a few extended beyond this range (Fig. 2). The lowest and highest temperatures examined were 12°C and 38°C, respectively. Prefeeding and feeding durations showed little variation with temperature but increased across developmental stage, with mean (standard deviation) values of 5.36 (0.82), 6.93 (0.71), and 8.07 (0.87) days for the prefeeding period, and 4.25 (0.63), 5.01 (0.72), and 8.21 (1.09) days for the feeding period in larvae, nymphs, and adults,

respectively (Table S1). In contrast, premoulting, preoviposition, oviposition, and incubation periods decreased markedly with increasing temperature, but their variations were more pronounced at lower temperatures. The fitted exponential functions captured these relationships well, with an average coefficient of determination (R^2) of 0.84. The estimated means and standard deviations of developmental durations for the temperature-independent substages, together with the fitted equations for the temperature-dependent developmental durations, are presented in Table S1.

Interstadial developmental durations predicted under field temperatures

Monthly average temperatures experienced under field conditions followed the expected latitudinal trend, with higher temperatures at lower latitudes (Fig. 3A). A notable exception was Xiaowutai, where temperatures were lower than expected for its latitude, likely because of its high elevation (839 meters). Across locations with field observations of tick seasonality, seasonal temperature variation was more pronounced in winter than in summer.

To validate the interstadial developmental duration model, we compared the predicted durations with field observations from Xiaowutai, China [12]. Although interpolating daily temperatures from monthly means may have introduced some bias, the predicted interstadial developmental durations closely matched the field-observed values (Fig. S8).

Across all study locations, the adult-to-larva transition, which encompasses egg laying and hatching, had the longest developmental duration, followed by the nymph-to-adult and larva-to-nymph transitions. The latter two had similar durations during summer, but the larva-to-nymph duration was remarkably shorter during winter (Figs. 3B and S9). All developmental durations were shortest from late spring through summer, decreasing gradually from January until May or June for the adult-to-larva transition, and until July or August for the nymph-to-adult and larva-to-nymph transitions, before increasing sharply in the fall due to rapid temperature declines (Figs. 3B and S9). These turning points occurred earlier at cooler locations (e.g., Xiaowutai and Gangwon 1) and later at warmer ones (e.g., Boso Peninsula and Haikou). Across the 1,000 simulations, uncertainty in the predicted developmental durations was greater during seasonal transition months and lower during summer and the winter diapause period (Fig. S9). Across scenarios with different mean questing durations, the estimated interstadial developmental durations increased with longer questing durations as expected, but the 95% confidence intervals derived from 1,000 simulations overlapped across all scenarios for every month and location (Figs. S10-12).

Full-generation developmental durations predicted under field temperatures

Under the baseline scenario (mean questing duration = 22 days, threshold for diapause onset = 11.5 hours, and threshold for diapause termination = 12.5 hours), for locations with tick seasonality data, predicted full-generation developmental durations were generally close to one year (Fig. 4), with slightly

longer durations at higher latitudes (Fig. S13). At some locations, such as Shandong and Hefei, predicted durations were shorter than one year when nymphal activity began in April or May, potentially explaining the small nymphal peak observed in fall (Figs. 1B and S7). Xiaowutai was an exception, with predicted durations ranging from 448 days when nymphal activity began in April–July, to 819 days when it began in October. A similar pattern was found in SFTS-endemic regions, where predicted durations were also approximately one year, but were short at some locations with higher temperature, including Xinyang, Miyazaki, and Taizhou, when nymphal activity began in April or May. In contrast, at locations where *H. longicornis* has not been reported, predicted full-generation developmental durations were consistently shorter than one year (Fig. 4).

As daily mean temperatures increased over time with global warming (Fig. S14), full-generation developmental durations decreased accordingly, with the greatest reductions occurring at higher latitudes (Fig. S15). On average, estimated full-generation developmental durations for nymphal activity beginning between April and June, corresponding to the observed period of peak nymphal activity, decreased by 5.90 days per decade at locations above 35° N, compared with a more modest decrease of 3.21 days per decade at locations below 25° N. These reductions were relatively small during summer, but more pronounced in spring and fall, particularly in April and October (Fig. S15).

When comparing scenarios with different mean questing durations, the estimated full-generation developmental durations increased with longer questing durations (Fig. S16). The overall pattern, in which locations with reported *H. longicornis* occurrence or human SFTS cases had full-generation developmental durations close to one year, whereas locations without reported *H. longicornis* occurrence had durations shorter than one year, persisted under the 12- and 32-day scenarios, although the number of locations with durations shorter than one year increased. Under the 42-day scenario, most locations had full-generation developmental durations longer than one year, whereas those at lower latitudes had durations close to one year (Fig. S16). However, this scenario appears less plausible because the predicted larval peak from the adult peak under this scenario tended to occur remarkably later than the observed peak, failing to capture the observed fall larval peak (Fig. S21).

When comparing different daylength thresholds for diapause onset and termination, the estimated full-generation developmental durations increased when diapause began earlier in fall or terminated later in spring, both of which corresponded to longer daylengths (Figs. S17-18). The effect of diapause onset thresholds was more pronounced for nymphal activity started in fall, while the effect of diapause termination thresholds was more pronounced for nymphal activity beginning in spring (Figs. S17-18). Under the 12.5-hour diapause onset or 13.5-hour diapause termination scenarios (timing represented by the darkest blue and red vertical lines in Fig. 5), full-generation developmental durations could approach or even exceed one year across all locations, including those with no reported *H. longicornis* occurrence. However, these scenarios are unlikely to reflect actual tick phenology, as tick activity continued after daylength dropped below 12.5 hours in fall (dark orange vertical line in Fig. 5), and began before daylength exceeded 13.5 hours in spring (dark blue vertical line in Fig. 5) at almost all locations with reported seasonal activity of *H. longicornis* (Fig. 5).

Inferred cohort structure of H. longicornis populations

Integrating observed seasonal activity with estimated interstadial developmental durations based on location-specific daily temperature profiles revealed that a single seasonal activity peak may comprise multiple cohorts. For example, the nymphal activity peak observed between March and June likely consisted of two cohorts. Nymphs questing in spring and early summer, approximately prior to May or June, depending on the mean questing duration scenario, likely molted in the previous year, entered behavioral diapause, and resumed questing in the current spring (Fig. 5, arrows from Larva to Nymph2 pointing to an earlier month, indicating a transition into the second year). In contrast, nymphs questing after June may have originated from larvae making up the smaller peak occurring earlier in the same spring (indicated by arrows pointing to a later month within the same year from Larva to Nymph2). For instance, at Gyeonggi-do 1, KR (Mugap-ri, Gwangju-si, Gyeonggi-do, South Korea, Table S1), the earliest larval activity began in April, and these larvae were predicted to develop into nymphs in June or later.

The adult activity peak, observed between June and August, also likely comprised two cohorts. Since nymphs questing in spring cannot complete development to adults before May even under the shortest questing duration scenario, adults observed before this month likely molted in the previous year and resumed questing in the current year. For example, in New York, the earliest questing nymphs were collected in March (Figs. 5 and S7), which would not complete development to adults until June. Consequently, adults active before this period were most likely overwintering individuals.

Larval activity typically exhibited two distinct peaks, with a major peak in August to September and a smaller peak in May. The major larval peak likely originated from adults that fed earlier in the same year (Fig. 5, illustrated by arrows connecting nymphs, adults, and larvae within a single year). In contrast, the smaller spring peak likely originated from adults that fed late in the previous season after August, when insufficient time remained for them to develop into questing larvae before temperatures and daylengths became unfavorable. These individuals likely completed development during the following spring and contributed to the spring larval peak.

At some locations, the entire generation could be completed within one year. For example, at the Boso Peninsular in Japan and Hefei in China, nymphs emerging in March-April developed into adults by May-June and subsequently produced larvae by August-September, which then may develop into questing nymphs again in September-October (Fig. 5). At some other locations, only nymphs that fed early in the spring could complete the whole generation within one year, whereas those feeding later could not. For instance, in Gangwon, nymphs questing in March-April developed into adults by June and larvae by September, which subsequently became active nymphs in the following spring. In contrast, the nymphs questing in May developed into adults in July, leaving insufficient time to produce active larvae and complete the generation within the same year (Fig. 5). At Xiaowutai, each generation requires at least two years because of its relatively low temperatures. Nymphs questing in spring developed into adults by summer and subsequently entered diapause either before or after feeding. Individuals that successfully

fed produced larvae the following spring, whereas those that failed to feed resumed activity as adults in following spring and contributed to the larval peak in the fall.

The above results remained consistent across mean questing scenarios, although the duration of each interstage transition increased slightly (Figs. S19-21).

Implications for SFTS transmission

Although *H. longicornis* exhibits broadly similar seasonal activity across locations (Fig. 1B), the seasonality of reported human SFTS cases varies substantially (Fig. 6). In China, for example, the peak month of human cases shifts geographically from July in Liaoning Province to June in Shandong Province, and to May in Henan, Jiangsu, Anhui, and Hubei, the provinces with the highest SFTS incidence (Fig. 6A). In South Korea, most locations showed peak incidence between August and October (Fig. 6B), whereas in Japan, peak incidence occurred as early as May in some prefectures and as late as October in others (Fig. 6C).

This variation suggests that human cases may involve different tick stages and cohorts across regions, with important implications for identifying the appropriate lag period and critical exposure window when assessing the effects of climatic factors on human SFTS risk. For example, in Gangwon, South Korea, human cases peaked in October, approximately one month after the larval activity peak in September, consistent with an incubation period of 5–14 days between tick exposure and disease onset. Since larvae questing in September developed from adults that fed in May and June (Fig. 5), climatic conditions affecting adult feeding success in May and June (e.g., the number of rainy days), oviposition in June and July (e.g., temperatures of 20–30°C and relative humidity of 90–100%, under which peak egg production per unit body weight was observed [26]), egg hatching from July to September (e.g., temperatures of 28–32°C and saturation deficit of 2–6 mm Hg [18]), and larval survival in September (e.g., temperatures around 28°C and saturation deficit below 2 mm Hg [19]) should be considered when predicting human SFTS risk. In contrast, in Shandong, the peak in human SFTS cases occurred in June, coinciding with high nymphal and adult activity in May and June. These nymphs and adults originated from larvae and nymphs that fed earlier in spring, respectively (Fig. 5). Therefore, climatic conditions affecting feeding success and survival during early spring are likely to be more relevant when evaluating human SFTS risk in this region.

Discussion

Human SFTS risk is closely associated with the abundance of infected ticks. Understanding tick phenology is therefore central to understanding the temporal distribution of human cases. Here, we integrated climatic data, laboratory-derived relationships between temperature and developmental durations, and field observations of *H. longicornis* seasonal activity to characterize similarities and differences in tick seasonality across diverse geographic locations and to explore the mechanisms and cohort structures underlying these patterns.

Despite substantial variations in temperature ranges across locations (Fig. 3A), remarkably consistent stage-specific seasonal patterns of *H. longicornis* were observed, with nymphs occurring mainly between March and June, adults between April and September, and larvae between August and October (Fig. 1B). Secondary peaks were also observed at some locations, including minor larval peaks in April-May and nymphal peaks in September-October. However, these secondary peaks were substantially smaller than the dominant peaks, potentially owing to differences in overwinter survival among life stages. For example, a field study in southwestern Virginia found that the overall overwinter survival rates for larvae, nymphs and adults were 2%, 98% and 59%, respectively [27]. The strong survival advantage of nymphs may contribute to the synchronization of population dynamics across regions, with populations predominantly overwintering as nymphs, resuming questing in spring, and subsequently progressing through the adult and larval stages. This life-history strategy could help maintain a consistent sequence of nymph, adult, and larval activity peaks despite substantial climatic heterogeneity.

Interestingly, despite substantial differences in annual mean temperature among the study locations (e.g., 10.6°C in Gangwon, South Korea vs. 17.2°C in Boso Peninsula, Japan), predicted full-generation developmental durations remained close to one year in most locations, possibly due to the fact that temperature differences are greatest during winter when ticks are in diapause and not actively questing, whereas temperatures during the active season are more similar. For instance, the mean temperature difference between Gangwon and the Boso Peninsula was on average 11.5°C from November to February but only 3.1°C from April to September. In addition, the developmental rates of ticks became less sensitive to temperature at higher temperatures (Fig. 2). For example, for nymphs beginning to quest on April 15th, the estimated time required to develop into adults was 66 days in the Boso Peninsula and 73 days in Gangwon (Fig. 3B), despite a 4.7°C lower monthly mean temperature in Gangwon. Together with the high overwinter survival rate of unfed nymphs, these factors may facilitate a predominantly one-year life cycle across diverse environments. Xiaowutai was the main exception among the study locations. Its annual mean temperature was 7.3°C, only 3.3°C lower than that of Gangwon. However, since developmental durations increased rapidly as temperature dropped below approximately 15°C (Fig. 2), even small temperature differences could lead to substantial developmental delays. For example, the estimated interstadial developmental duration from adults beginning to quest on June 15th to the subsequent larval stage was 89.9 days in Gangwon, but increased to 180.8 days in Xiaowutai. When combined with the later onset of nymphal activity and slightly longer development from nymphs to adults, this delay prevented the transition from adults to larvae from being completed within the same year as the preceding nymph-to-adult transition. As a result, the estimated full-generation duration in Xiaowutai extended beyond one year.

In locations where *H. longicornis* has not been reported, the estimated full-generation duration was often substantially shorter than one year under most examined scenarios (Figs. 4, S10-12). This pattern may potentially be associated with reduced overwinter survival if tick populations are less able to maintain a stable overwintering nymphal stage. However, this interpretation should be treated with caution, as the estimated full-generation duration approached one year or even extended over one year under scenarios with longer mean questing durations or higher daylength thresholds for diapause onset and termination.

Further studies are needed to determine whether the absence of reported *H. longicornis* populations in these locations reflects environmental conditions unsuitable for the species or simply its failure to expand into these areas to date.

Although temperatures have increased over time due to global warming (Fig. S14) to a similar extent across the studied locations, the resulting changes in full-generation developmental durations were more pronounced in colder regions and during colder months (Fig. S15), probably due to the nonlinear temperature dependence of development, where developmental durations decrease more rapidly with increasing temperature at lower temperature ranges, but change more gradually at higher temperatures (Fig. 2).

Our findings of two distinct larval activity peaks corresponding to two separate cohorts, as well as single nymphal and adult activity peaks comprising two cohorts each, are consistent with a study conducted in New Jersey ("New Jersey 1, US" in our study) that used stored lipid content to infer the phenological age of *H. longicornis* [16]. However, the inferred timing of cohort transitions for nymphs and adults differed between the two studies. In our study, the new nymphal cohort emerged in June, originating from the spring larval peak, whereas the stored lipid study inferred that new nymphs became active in April after developing from engorged larvae that had overwintered [16]. Similarly, in our study, the new adult cohort emerged in May from nymphs that had fed during the same year, alongside adults that had overwintered. In contrast, the stored lipid study inferred the co-occurrence of two adult cohorts with different lipid levels, with high-lipid cohort originating from nymphs that fed later in the previous season and the low-lipid cohort from nymphs that fed earlier [16]. The findings of the stored lipid study should be interpreted cautiously because lipid content was not standardized by reduced dry weight, as strongly recommended in previous literature [15]. Ticks of different body sizes, as reflected by reduced dry weight, have different baseline lipid levels, and they also tend to terminate diapause at different time points [15]. Therefore, accounting for body size is important to avoid biased inferences about cohort structure. Moreover, previous field studies suggest that larvae rarely survive winter [27], further challenging the interpretation that nymphs active in April originated from overwintered engorged larvae. Future studies of the overwintering strategies of *H. longicornis*, together with lipid analyses that account for body size, are needed to better characterize the timing of transitions between cohorts within each activity peak.

Although *H. longicornis* seasonality was broadly similar across locations, the seasonality of human SFTS cases varied substantially among regions. One notable example is the October peak of human SFTS cases observed in several regions of South Korea, including Gyeonggi, Seoul, and Chungbuk, which may reflect differences in human-tick contact patterns. The timing of human exposure to ticks may vary with agricultural activities. In these regions, sweet potatoes and scallions are among the major crops and are harvested mainly in September and October, whereas the agricultural busy periods in SFTS-endemic areas of China are typically concentrated in May and August [28]. Moreover, high tick abundance has been reported in sweet potato and scallion fields in Gyeonggi, with a minimum SFTSV infection rate of 0.25% [29]. Another possible explanation is the prolonged fall activity of *H. flava* in South Korea. However, its contribution to human SFTS transmission is likely limited, given that *H. longicornis* accounts

for approximately 95% of ticks collected in South Korea [30, 31, 32]. These findings highlight that similar tick phenology does not necessarily translate into similar human SFTS seasonality. Therefore, models of human SFTS risk should account for both location-specific tick activity and temporal patterns of human-tick contact.

We also found that the geographic coverage of existing field observations of *H. longicornis* seasonality remained limited (Fig. 1A). Although China contributed over 99 percent of all reported SFTS cases globally, the seasonality of *H. longicornis* in major SFTS transmission hotspots, including the Dabie Mountain region and Liaoning Province, remains largely uncharacterized. While one study collected data for Shandong Province [33], its findings differ remarkably from other locations, with a larval activity peak observed in May rather than August-September (Fig. 1B). Moreover, the corresponding nymphal peak expected from this larval peak was not observed, raising concerns about the representativeness or quality of these data. In Japan, existing field studies are also geographically distant from major SFTS transmission hotspots in the eastern part of the country (Fig. 1A). In contrast, South Korea has contributed the majority of high-quality field observations available for this analysis. Future studies should prioritize filling these geographic gaps, particularly in major SFTS transmission hotspots.

Similarly, most previous laboratory studies have focused on temperatures between 20 and 30°C (Fig. 2), with limited observations outside this range, particularly at lower temperatures where developmental durations change rapidly with temperature. This data scarcity limits the precision of the estimated exponential relationships between temperature and developmental duration and may introduce uncertainty when estimating developmental durations during early spring and late fall, when temperatures are below 20°C, but ticks remain active. Additional laboratory experiments under low temperatures would therefore substantially improve the characterization of temperature-dependent development.

Our study has several limitations. First, we focused exclusively on *H. longicornis*, since it is the dominant tick species in SFTS transmission hotspots [32, 34]. However, the methodological framework developed here could be readily extended to other tick species. Second, we considered only temperature and did not explicitly incorporate other climatic factors, such as humidity. Since interstadial developmental durations were primarily temperature-dependent and varied little across humidity levels (Fig. S2), temperature alone may be sufficient when the primary objective is to estimate developmental durations. However, humidity plays a critical role in determining tick survival [17, 18, 19], and should therefore be incorporated into studies aiming to explain seasonal variation in stage-specific abundance. Third, we used daily temperature data from the ERA5 reanalysis dataset at a spatial resolution of approximately 9×9km, which may not adequately capture the microclimatic conditions experienced by ticks. Future field studies should therefore aim to collect site-specific climatic data, particularly near the soil surface. Finally, although the model for interstadial developmental durations was partially validated against field observations, the inferred cohort structures were not directly validated. Future studies could incorporate quantitative approaches, such as lipid analysis, to provide independent validation and further insights into cohort structure, especially in the SFTS transmission hotspots.

Conclusion

In conclusion, by integrating data from multiple sources within an empirical quantitative framework, we identified broadly consistent seasonal activity patterns of *H. longicornis* across diverse climatic conditions, together with relatively modest geographic variation in interstadial and full-generation developmental durations and cohort structures underlying these activity patterns. In contrast, human SFTS seasonality varied substantially among regions, highlighting the importance of location-specific lags between environmental factors and human cases and of temporal variation in human-tick contact when modelling human SFTS risk. Future studies should prioritize field surveys of *H. longicornis* seasonality in major SFTS transmission hotspots and apply quantitative approaches, such as lipid analysis, to better characterize the cohort structures underlying observed seasonal activity.

Abbreviations

SFTS: Severe fever with thrombocytopenia syndrome;

SFTSV: Severe fever with thrombocytopenia syndrome virus;

CNKI: China National Knowledge Infrastructure;

CN: China;

JP: Japan;

KR: South Korea;

US: United States.

Declarations

Acknowledgements

The computation is completed in the HPC Platform of Huazhong University of Science and Technology.

Funding

This work was supported by the National Natural Science Foundation of China (82204110 and 82674740).

Availabibility of data and materials

All data generated or analyzed during this study are included in this published article and its supplementary information files.

Author’s contributions

QC designed the study, conducted the systematic review of responses of *H. longicornis* to temperature and humidity under laboratory conditions, analyzed the data, and wrote the manuscript. QL validated the *H. longicornis* seasonality data. MH conducted the systematic review of *H. longicornis* seasonality and extracted the data. All authors substantially revised the manuscript and read and approved the final version.

Ethics approval and consent to participate

Not applicable.

Consent for publication

Not applicable.

Competing interests

The authors declare that they have no competing interests.

References

1. Yu X-J, Liang M-F, Zhang S-Y, Liu Y, Li J-D, Sun Y-L, et al. Fever with thrombocytopenia associated with a novel bunyavirus in China. New England Journal of Medicine. 2011;364 16:1523–32.
2. Zheng W, Zhong F, Wang W, Liu H, Peng Y, Carr MJ, et al. SFTS exerts an underrecognized disease burden and socioeconomic effect in East Asia. Biosafety and Health. 2026;8 01:15–9.
3. Cui H, Shen S, Chen L, Fan Z, Wen Q, Xing Y, et al. Global epidemiology of severe fever with thrombocytopenia syndrome virus in human and animals: a systematic review and meta-analysis. The Lancet Regional Health–Western Pacific. 2024;48.
4. DU Shanshan S, CHEN X, LIU H, ZHANG L, HUANG X. Epidemiological characteristics of severe fever with thrombocytopenia syndrome in China from 2010 to 2023. Chinese Journal of Schistosomiasis Control. 2025;37 4:371.
5. Korea Centers for Disease Control and Prevention: South Korea Infectious Diseases Surveillance Yearbook 2013. 2013.

6. Korea Centers for Disease Control and Prevention: South Korea Infectious Diseases Surveillance Yearbook 2024. 2024.
7. Japan Institute for Health Security: The Infectious Disease Information Website. https://id-info.jihs.go.jp/niid/en/data/6199-idwr-sokuho-data-e-1553.html (2025). 2026.
8. Woo D, Michelow IC, Choi Y, Lee H, Park S. Transmission of Severe Fever with Thrombocytopenia Syndrome (SFTS) to humans: A systematic review of individual participant data and meta-analysis. Journal of Infection and Public Health. 2025;18 6:102685.
9. Luo L-M, Zhao L, Wen H-L, Zhang Z-T, Liu J-W, Fang L-Z, et al. *Haemaphysalis longicornis* ticks as reservoir and vector of severe fever with thrombocytopenia syndrome virus in China. Emerging infectious diseases. 2015;21 10:1770.
10. Zhao L, Li J, Cui X, Jia N, Wei J, Xia L, et al. Distribution of *Haemaphysalis longicornis* and associated pathogens: analysis of pooled data from a China field survey and global published data. The Lancet Planetary Health. 2020;4 8:e320-e9.
11. Hu Y-Y, Zhuang L, Liu K, Sun Y, Dai K, Zhang X-A, et al. Role of three tick species in the maintenance and transmission of severe fever with thrombocytopenia syndrome virus. PLoS Neglected Tropical Diseases. 2020;14 6:e0008368.
12. Zheng H, Yu Z, Chen Z, Zhou L, Zheng B, Ma H, et al. Development and biological characteristics of *Haemaphysalis longicornis* (Acari: Ixodidae) under field conditions. Experimental and Applied Acarology. 2011;53 4:377–88.
13. Shin HJ, Jeong JY, Hong CE, Lee H, Lee KW, Lee W-G, et al. Long-term ecological surveillance of hard ticks (Acari: Ixodidae) and SFTSV in Dangjin, central Korea (2018–2024). 2025.
14. Cumbie AN, Whitlow AM, Arneson A, Du Z, Eastwood G. The Distribution, Seasonal Abundance, and Environmental Factors Contributing to the Presence of the Asian Longhorned Tick (*Haemaphysalis longicornis*, Acari: Ixodidae) in Central Appalachian Virginia. Journal of Medical Entomology. 2022;59 4:1443–50; doi: 10.1093/jme/tjac067. https://doi.org/10.1093/jme/tjac067.
15. Randolph SE, Green RM, Hoodless AN, Peacey MF. An empirical quantitative framework for the seasonal population dynamics of the tick Ixodesricinus. International Journal for Parasitology. 2002;32 8:979–89; doi: https://doi.org/10.1016/S0020-7519(02)00030-9. https://www.sciencedirect.com/science/article/pii/S0020751902000309.
16. Bickerton M, González J, Toledo A. Insights on the phenology of the Asian longhorned tick (*Haemaphysalis longicornis*) using stored lipids. Insect Science. 2026;33 1:396–406; doi: https://doi.org/10.1111/1744-7917.70009. https://doi.org/10.1111/1744-7917.70009.
17. Yano Y, Shiraishi S, Uchida T. Effects of humidity on development and growth in the tick, *Haemaphysalis longicornis*. 1988.
18. Heath A. The temperature and humidity preferences of *Haemaphysalis longicornis*, *Ixodes holocyclus* and *Rhipicephalus sanguineus* (Ixodidae): studies on eggs. International journal for parasitology. 1979;9 1:33–9.

19. Heath A. The temperature and humidity preferences of *Haemaphysalis longicornis*, *Ixodes holocyclus* and *Rhipicephalus sanguineus* (Ixodidae): studies on engorged larvae. International journal for parasitology. 1981;11 2:169 – 75.
20. Randolph SE. Abiotic and biotic determinants of the seasonal dynamics of the tick *Rhipicephalus appendiculatus* in South Africa. Medical and Veterinary Entomology. 1997;11 1:25–37; doi: https://doi.org/10.1111/j.1365-2915.1997.tb00286.x. https://doi.org/10.1111/j.1365-2915.1997.tb00286.x.
21. Rubino FI, Pascoe E, Barrand ZA. Spring fever: early spring predicts *Ixodes pacificus* (Acari: Ixodidae) activity in northwestern California. Journal of Medical Entomology. 2025;62 4:938–47.
22. Fujimoto K. Effect of photoperiod on the host attachment and development in the tick, *Haemaphysalis longicornis*. Medical Entomology and Zoology. 1995;46 4:345–8; doi: 10.7601/mez.46.345.
23. González J, Fonseca DM, Toledo A. Effect of short photoperiod on the development of *Haemaphysalis longicornis* (Ixodida: Ixodidae). Journal of Medical Entomology. 2024;61 2:504–7; doi: 10.1093/jme/tjad171. https://doi.org/10.1093/jme/tjad171.
24. Forsythe WC, Rykiel EJ, Stahl RS, Wu H-i, Schoolfield RM. A model comparison for daylength as a function of latitude and day of year. Ecological Modelling. 1995;80 1:87–95; doi: https://doi.org/10.1016/0304-3800(94)00034-F. https://www.sciencedirect.com/science/article/pii/030438009400034F.
25. Zheng H, Yu Z, Zhou L, Yang X, Liu J. Seasonal abundance and activity of the hard tick *Haemaphysalis longicornis* (Acari: Ixodidae) in North China. Experimental and applied acarology. 2012;56 2:133–41.
26. Yano Y, Shiraishi S, Uchida T. Effects of temperature on development and growth in the tick, *Haemaphysalis longicornis*. Experimental & applied acarology. 1987;3 1:73–8.
27. Whitlow AM, Schürch R, Mullins D, Eastwood G. The Influence of Southwestern Virginia Environmental Conditions on the Potential Ability of *Haemaphysalis longicornis*, *Amblyomma americanum*, and *Amblyomma maculatum* to Overwinter in the Region. 2021.
28. Qiu B, Wu F, Hu X, Yang P, Wu W, Chen J, et al. A robust framework for mapping complex cropping patterns: The first national-scale 10 m map with 10 crops in China using Sentinel 1/2 images. ISPRS Journal of Photogrammetry and Remote Sensing. 2025;224:361–81; doi: https://doi.org/10.1016/j.isprsjprs.2025.04.012. https://www.sciencedirect.com/science/article/pii/S0924271625001480.
29. Kim H, Kim D, Park J, Park N. Genotype analysis of severe fever with thrombocytopenia syndrome virus (SFTSV) detected in field-collected ticks from patient-associated sites in South Korea. Korean J Microbiol. 2025;61 4:267–73; doi: 10.7845/kjm.2025.5069. http:///journal/view.html?doi=10.7845/kjm.2025.5069.
30. Noh BE, Kim H, Ju JW, Lee HI. Surveillance of Tick Density in the Republic of Korea, 2022. Public Health Weekly Report. 2023;16 32:1119–30; doi: 10.56786/phwr.2023.16.32.1.

31. Noh B-E, Kim H, Ju J-W, Lee H-I. Surveillance of Tick Population in the Republic of Korea, 2023. Public Health Weekly Report. 2024;17 33:1406-18; doi: 10.56786/PHWR.2024.17.33.2. https://phwr.org/journal/view.html?doi=10.56786/PHWR.2024.17.33.2.
32. Lee HS, Noh B-E, Ju J-W, Lee H-I. Surveillance of Tick Populations in the Republic of Korea in 2024. Public Health Weekly Report. 2025;18 31:1168-83; doi: 10.56786/PHWR.2025.18.31.2. https://phwr.org/journal/view.html?doi=10.56786/PHWR.2025.18.31.2.
33. Han Y, Yin H, Liu Y, Cao X, Sun Q, Cai T, et al. Comprehensive characterization of ecological features and spatiotemporal distribution patterns of ticks in Shandong Province, China (2021–2023). Parasites & Vectors. 2025;18 1:460; doi: 10.1186/s13071-025-07055-9. https://doi.org/10.1186/s13071-025-07055-9.
34. Wu H, Liu X, Yue Y, Ren D, Wang J, ZHao C, et al. National surveillance report on ticks in China, 2019. Chinese Journal of Vector Biology and Control. 2020;31 4:417–22.

Figures

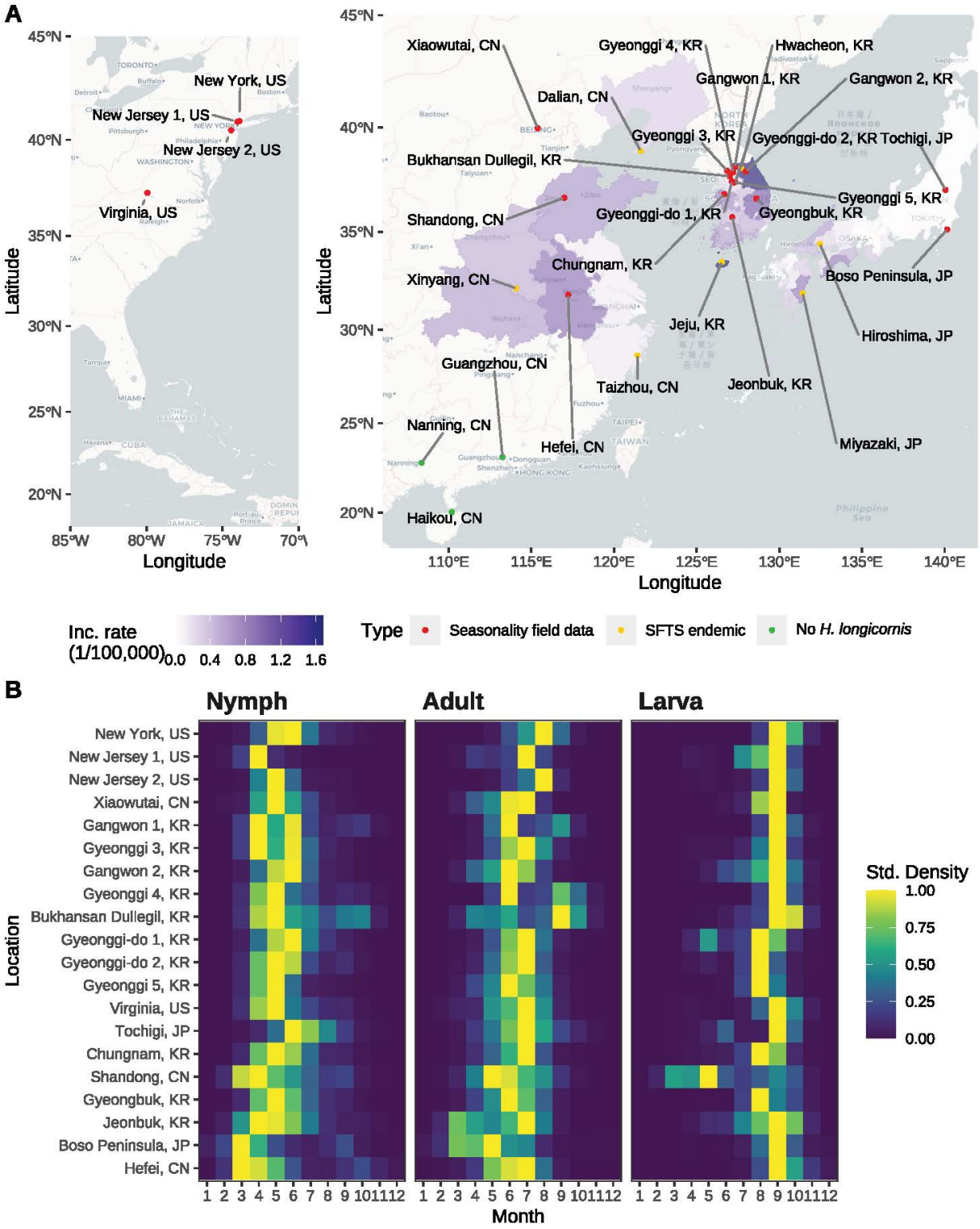

Figure 1

Geographic distribution of study locations and seasonality of *H. longicornis*. (A) Locations of surveyed sites (red dots), along with additional locations considered, including SFTS transmission hotspots (orange dots) and locations without known *H. longicornis* presence (green dots). The background shading represents reported average annual SFTS incidence rates at the first administrative level, with dark blue indicating higher incidence rate and white indicating lower incidence rate. (B) Seasonal activity

patterns of free-living *H. longicornis* nymphs, adults and larvae. For visualization, tick abundances at each site were normalized to a 0-1 scale, where 0 represents the minimum and 1 the maximum observed abundance. The original, non-normalized time series of tick abundances are provided in Fig. S7.

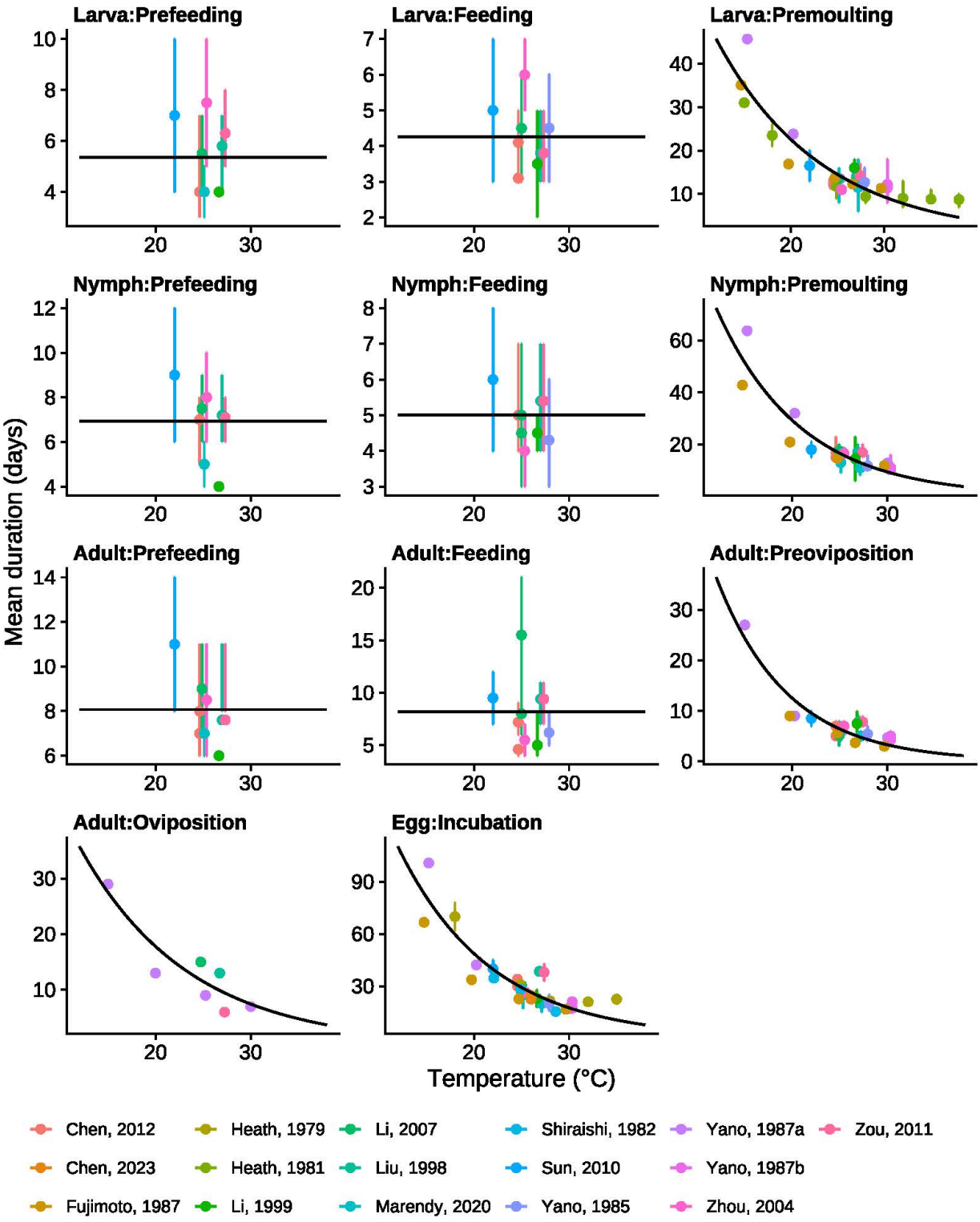

Figure 2

Mean developmental durations of *H. longicornis* at different temperatures, based on the data from published laboratory studies. Detailed data are provided in Table S3, and parameters of the fitted lines are provided in Table S1.

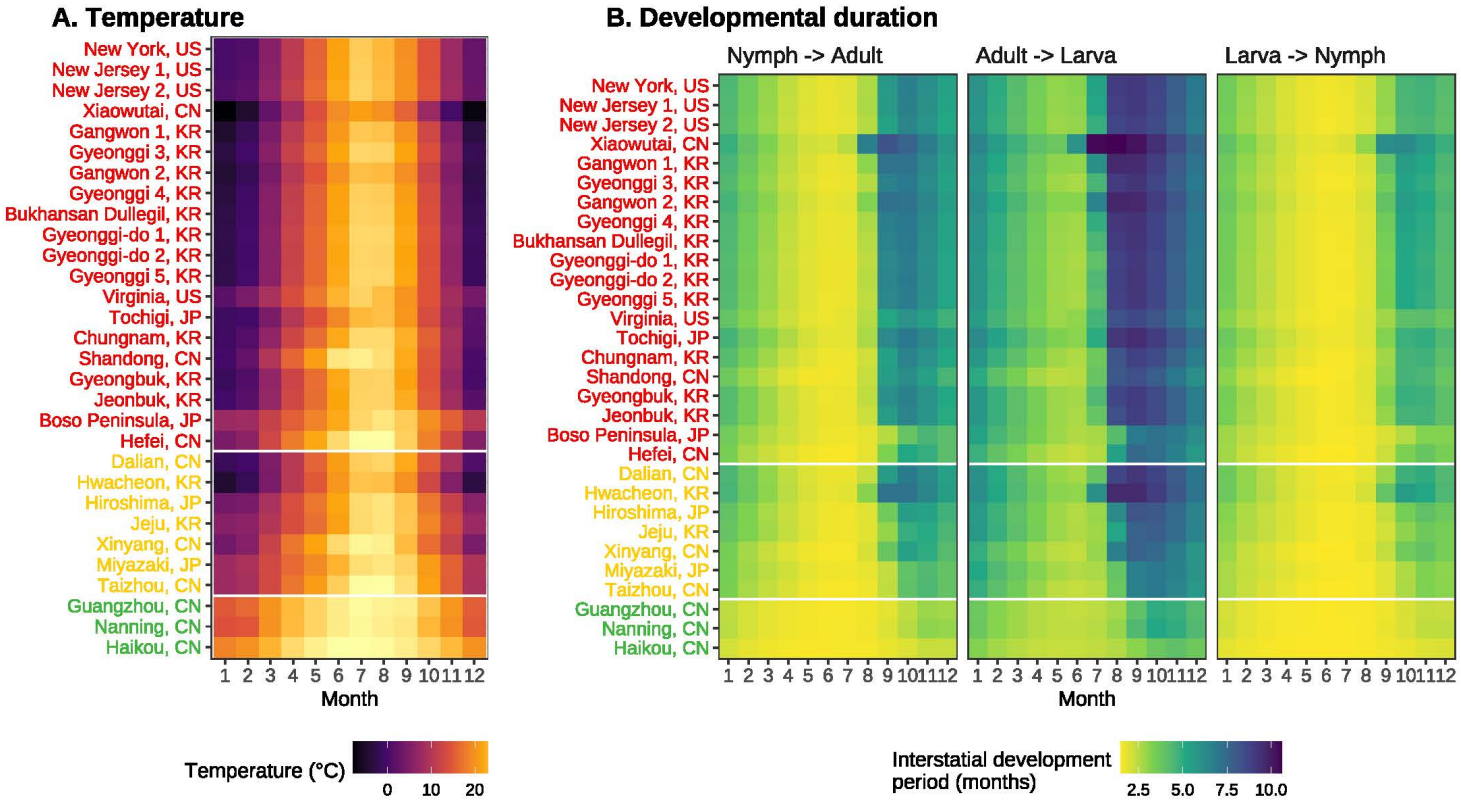

Figure 3

Temperature conditions and estimated interstadial developmental durations across study locations. (A) Monthly average temperatures from 2021 to 2025. (B) Mean interstadial developmental durations estimated using daily mean temperatures from 2021 to 2025. The number of days was divided by 30 to be converted into the number of months. Location names are color-coded: red indicates sites with tick seasonality surveillance data, yellow indicates SFTS transmission hotspots, and green indicates locations without reported *H. longicornis*presence. Within each category, locations were ordered by decreasing latitude from top to bottom.

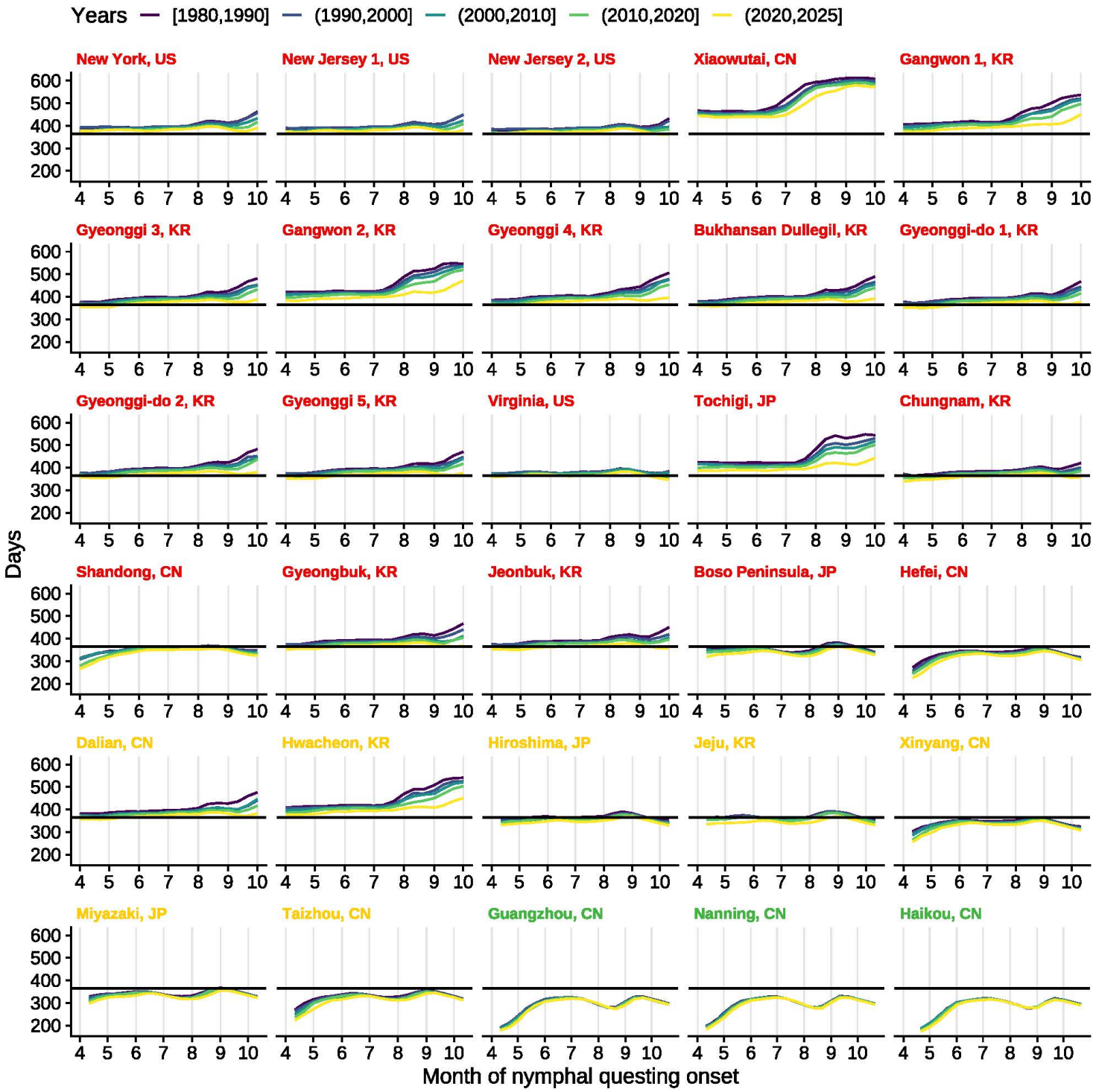

Figure 4

Full-generation developmental durations across all locations and decades by month of nymphal questing onset. The location names are color-coded: red indicates the locations with tick seasonality surveillance data, yellow indicates SFTS transmission hotspots, and green indicates locations without reported *H. longicornis*presence. Within each category, the locations were ordered by decreasing latitude. Horizontal lines represent a full year of 365 days.

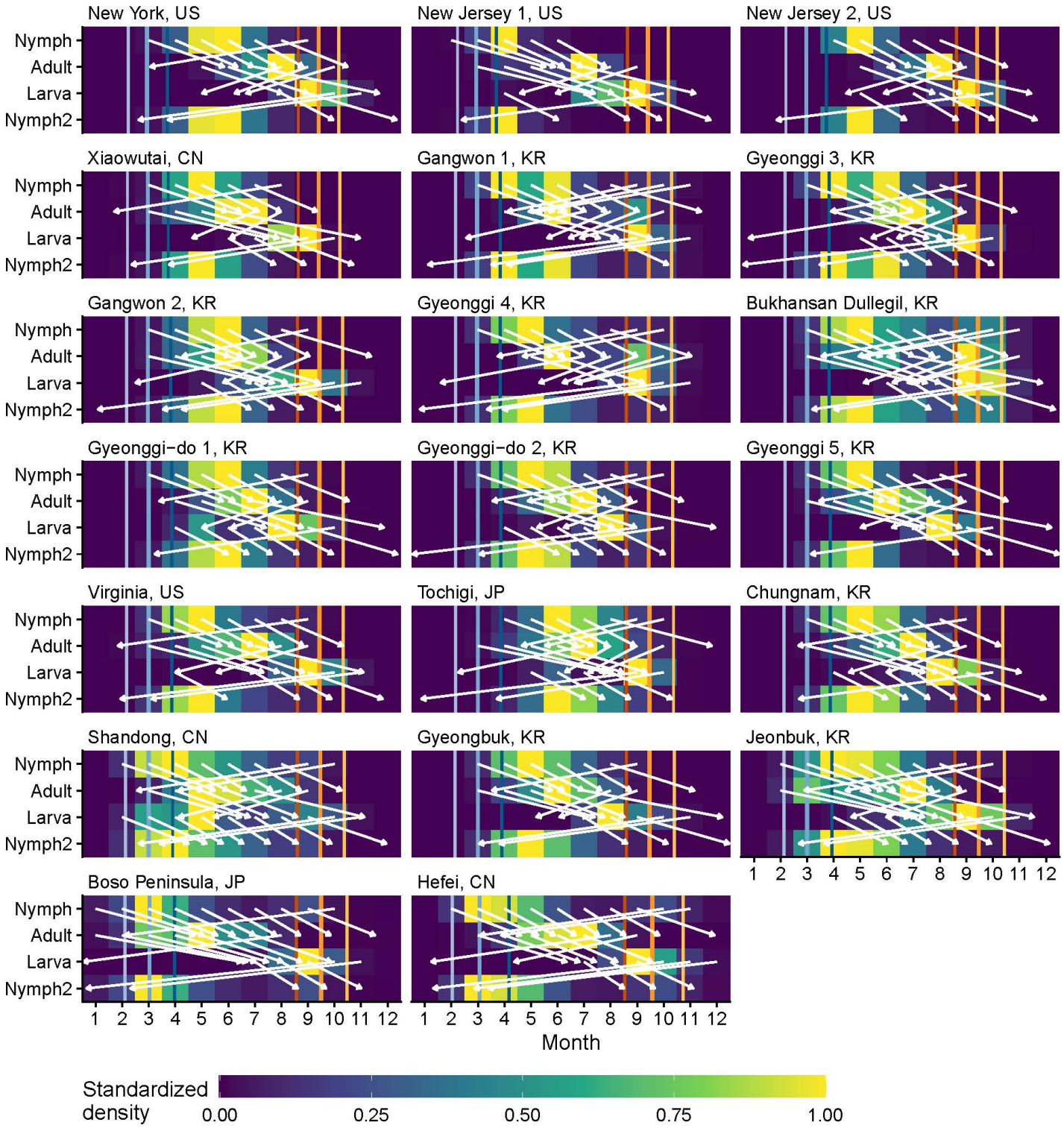

Figure 5

Interstadial developmental durations combined with observed seasonal activity of *H. longicornis* under a mean questing duration of 22 days. Tiles are colored according to life stage-specific tick abundance, averaged across all study years and rescaled to 0 to 1 using (x − min)/(max − min). Nymph2 on the y-axis means the second generation of nymphs. Arrows connect the midpoint of each month to the time when the subsequent life stage started feeding. Arrows originated from months contributing less than

5% of the annual abundance were omitted. Blue vertical lines indicate daylengths of 11.5, 12.5, and 13.5 hours (from left to right), representing the scenarios examined for diapause termination. Orange vertical lines indicate daylengths of 12.5, 11.5, and 10.5 hours (from left to right), representing the scenarios examined for diapause onset. Results for mean questing durations of 12, 32, and 42 days are presented in Figs. S19-21.

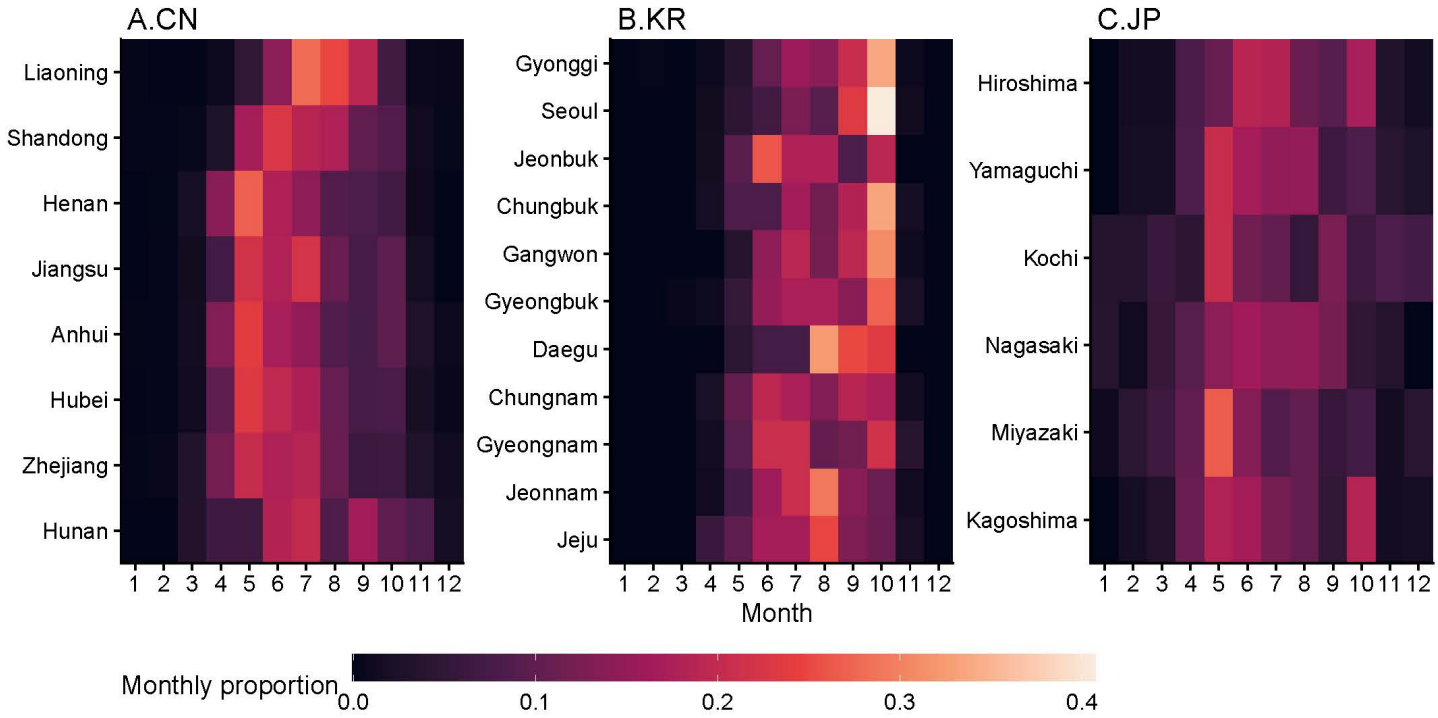

Figure 6

Monthly proportion of reported human SFTS cases by first-level administrative divisions, calculated as the number of cases reported in each month divided by the total number of cases reported over the entire study period, in (A) China, (B) South Korea, and (C) Japan. To ensure stable estimates of seasonal proportions, only first-level administrative divisions with at least 50 reported cases during the study period are shown.

Supplementary Files

This is a list of supplementary files associated with this preprint. Click to download.

- H.longicornisgenerationR0.1SIclean.docx